Noncovalent functionalization of graphene with end-functional polymers†

Eun-Young Choi,[ab] Tae Hee Han,[a] Jihyun Hong,[a] Ji Eun Kim,[a] Sun Hwa Lee,[a] Hyun Wook Kim[a] and Sang Ouk Kim*[a]

Received 14th September 2009, Accepted 27th November 2009
First published as an Advance Article on the web 20th January 2010
DOI: 10.1039/b919074k

Stable dispersion of reduced graphene in various organic solvents was achieved *via* noncovalent functionalization with amine-terminated polymers. An aqueous dispersion of reduced graphene was prepared by chemical reduction of graphene oxide in aqueous media and was vacuum filtered to generate reduced graphene sheets. Good solvents and nonsolvents for the dried reduced graphene were evaluated using a solubility test. To achieve stable dispersion in the evaluated nonsolvents, amine-terminated polystyrene was noncovalently functionalized to the graphene, while graphene sheets were phase transferred *via* sonication from aqueous phase to the organic nonsolvent phase, including the amine-terminated polymers. Thorough FTIR and Raman spectroscopy investigation verified that the protonated amine terminal group of polystyrene underwent noncovalent functionalization to the carboxylate groups at the graphene surface, providing the high dispersibility in various organic media.

Introduction

Graphene is an emerging carbon nanomaterial that is potentially useful in a variety of technological areas, such as electronics,[1–3] sensors,[4] electromechanics,[5] solar cells,[6,7] memory devices,[8] hydrogen storage[9,10] ultracapacitors,[11] and so on. Since the unexpected separation of single-layer graphene sheet from natural graphite through the laborious micromechanical cleavage method,[1] various synthesis methods for graphene have been developed, including epitaxial growth,[12] thermal exfoliation of graphite oxide,[13] gas phase synthesis,[14,15] chemical reduction from graphene oxide,[16–20] and liquid phase exfoliation of graphite.[21–23] Nevertheless, the mass production of highly functional, fully exfoliated graphene sheets still remains as a formidable challenge.

Oxidative exfoliation of natural graphite by acid treatment and subsequent chemical reduction has been evaluated as one of the most efficient methods for low-cost, large-scale production of graphene. Graphene oxide, an oxidized derivative of graphene generated in this approach, is readily dispersable in aqueous media. This aqueous dispersibility is greatly advantageous for processing graphene into films, sheets, composites and so on.[16–18,24–27] Ruoff and co-workers[16] prepared stable aqueous dispersion of polymer-coated reduced graphene by reducing graphene oxide sheets using hydrazine in the presence of poly(sodium-4-pyrene sulfonate).[17] Li *et al.*[18] demonstrated that a dispersant-free aqueous dispersion of reduced graphene can be prepared by maintaining a high pH value during chemical reduction and thus controlling electrostatic stabilization arising from negatively charged functional groups remaining at the reduced graphene surface.

Unlike aqueous dispersibility, the organo-dispersibility of graphene has been less explored so far. Haddon and co-workers[28] demonstrated that covalent functionalization with octadecylamine yields exfoliated graphene in organic solvents. Müllen and co-workers[29] produced chloroform-soluble graphene through surfactant-supported functionalization. Ruoff and co-workers[30] prepared an organosoluble polystyrene-graphene composite by means of chemical reduction with N,N-dimethylhydrazine of phenyl isocyanate-treated graphene oxide. Polymer-assisted organo-dispersion of graphene is particularly advantageous for preparing graphene-polymer nanocomposites with remarkably enforced electrical and mechanical properties.[30,31]

In this work, we exploited organo-dispersed graphene in various solvents mediated by noncovalent functionalization with end-functional polymers. First, an aqueous dispersion of reduced graphene was prepared by chemically reducing graphene oxide according to recently reported preparation method.[18] The dispersibilitiy of the dried reduced graphene was investigated in a broad spectrum of organic solvents. For the evaluated nonsolvents, the stable dispersion of graphene was achieved *via* noncovalent functionalization with amine-terminated, end-functional polymers. The carboxylate functional groups of reduced graphene remaining after chemical reduction acted as functionalization sites for the protonated terminal amine groups of the end-functional polymer. The noncovalent grafting *via* ionic interaction was confirmed by attenuated total reflection Fourier transform infrared (ATR-FTIR) and Raman spectroscopy.

Experimetal

Materials

Graphite was purchased from GK (product MGR 25 998 K). The hydrazine and ammonia for the reduction of graphene oxide were purchased from Junsei. H_2SO_4 (Merck), $KMnO_4$

[a]*Department of Materials Science and Engineering, KAIST, Daejeon, 305-701, Republic of Korea. E-mail: sangouk.kim@kaist.ac.kr*
[b]*Nuclear Fuel Cycle Group, Korea Atomic Energy Research Institute, Daejeon, 305-353, Republic of Korea*

† Electronic supplementary information (ESI) available: ATR-FTIR spectra, UV-Vis spectroscopy and thermogravimetric analysis. See DOI: 10.1039/b919074k

(Sigma-Aldrich) and H_2O_2 (Sigma-Aldrich) were used as received. o-Xylene, acetone, pyridine, 1-methyl-2-pyrrolidone (NMP), 1,3-dimethyl-2-imidazolidinone, N,N-dimethylformamide (DMF), γ-butyrolactone, dimethyl sulfoxide (DMSO), 1-propanol, ethanol (EtOH), methanol (MeOH) and ethylene glycol (EG) were purchased from Sigma-Aldrich. Hexane, benzene, tetrahydrofuran (THF), and dichloromethane were purchased from Junsei. End-functional polymers including amine terminated polystyrene (PS–NH_2) (M_w = 3,000 g mol^{-1}), carboxylic acid terminated polystyrene (PS–COOH) (M_w = 3,000 g mol^{-1}) and hydroxyl terminated poly(methyl methacrylate) (PMMA-OH) (M_w = 6,000 g mol^{-1}) were purchased from Polymer Source, Inc.

Preparation of reduced graphene

Graphite oxide was prepared by a modified Hummers method.[32] Dialysis of the as-prepared the graphite oxide was carried out to completely remove residual salts and acids. The gel-like graphite oxide was freeze-dried, and a fine brown powder was obtained. Aqueous graphene oxide dispersion of 0.1 wt% was prepared by mild sonication, yielding a homogeneous brown dispersion. The graphene oxide dispersion was further centrifuged to remove unexfoliated graphite oxide (15000 r.p.m., 10 min). The concentration of the remaining exfoliate dispersion was ~0.030 wt%. A reduced graphene dispersion was prepared by chemically reducing the aqueous graphene oxide dispersion. After the graphene oxide dispersion was heated in an oil bath at 100 °C under reflux, 15 μl of ammonia solution (28 wt% in water) and 30 μl of hydrazine (80 wt% in water) were added. After chemical reduction for 2 h, the obtained mixture was cooled to room temperature and excess hydrazine and ammonia were removed by dialysis. The resultant reduced graphene dispersion was centrifuged to remove flocculated aggregates caused by chemical reduction (15000 r.p.m., 10 min) and the concentration of the finally obtained dispersion was 0.0090 wt%. Graphene paper was made by vacuum filtration of the homogeneous dispersion through a polyvinylidene fluoride membrane filter (47 nm in diameter, 0.45 μm pore size; Millipore).

Preparation of polymer functionalized reduced graphene

End-functional polymers (0.10–2.0 wt%, 1 ml) were dissolved in organic solvents (dichloromethane, o-xylene, benzene, and hexane). The prepared organic polymer solution was added to the vial containing aqueous reduced graphene dispersion (0.0090 wt%, 1 ml). The vial including phase-separated organic and aqueous phases was subjected to 5 h sonication for the noncovalent functionalization and phase transfer of graphene.

Characterization of reduced graphene and polymer functionalized reduced graphene

ATR-FTIR analyses were performed with Bruker Optiks, IFS66V S^{-1}, where a microscope (HYPERION 3000) was fitted with an ATR objective as the internal reflectance element and a mercury-cadmium-telluride (MCT) detector. KBr pellet samples were used. The number of scans was 68, and the scanning resolution was 2 cm^{-1}. Atomic force microscopy (AFM) images of reduced graphene were taken in the tapping mode AFM (Nanoman, Veeco). Raman spectra were recorded from 1800 cm^{-1} to 100 cm^{-1} on a high resolution dispersive Raman microscope (LabRAM HR UV/Vis/NIR, Electrooptics). The dispersions of grapheme oxide and reduced graphene in aqueous or organic solvents were analyzed by UV-Vis spectroscopy (Shimadzu UV-VIS-NIR scanning spectrophotometer, UV-3101 PC).

Results and discussion

Dispersibility of reduced graphene in various organic solvents

An aqueous dispersion of reduced graphene was prepared by chemical reduction of graphene oxide in aqueous media without any dispersing agent. A detailed investigation on the chemical composition and physical properties revealed that the reduced graphene sheets decorated with chemical functionalities such as hydroxyl groups and carboxylic acid groups were dispersed in aqueous medium (ESI†). We also observed aqueous dispersion of reduced graphene shows long-term (several months) stability caused by negatively charged functional groups at the reduced graphene.[18] The electrical conductivity is a good indicator of the extent to which graphene oxide has been reduced. A graphene film was prepared by vacuum filtration and dried at 110 °C to evaporate any residual moisture for conductivity measurement. The average conductivity was measured to be about 1500 S m^{-1}. It indicates that the conjugated sp^2-carbon network is extensively restored in the reduced graphene.

The dispersibility of reduced graphene in various (16 kinds) organic solvents was tested in the following procedure. Firstly, dried graphene paper was prepared by vacuum filtration of the aqueous reduced graphene dispersion. A few pieces of the graphene paper and an organic solvent were loaded in a vial (reduced graphene concentration: 0.4 mg ml^{-1}) and sonicated for 5 h. The colloidal stability of the prepared dispersion was evaluated for 1 month. Fig. 1(a) shows the photographs of reduced graphene dispersions in water and various organic solvents 1 month after preparation. Black or grey colors of the vials indicate that the dried and reduced graphene can be dispersed in the corresponding solvents. The dispersibility in various solvents is summarized in Table 1. The reduced graphene formed a stable dispersion in NMP, 1,3-dimethyl-2-imidazolidinone, γ-butyrolactone, 1-propanol, DMF, EtOH and EG (a limited amount of precipitate was observed in these solvents). UV-Vis absorption spectroscopy was employed to confirm the dispersibility of the reduced graphene, as shown in Fig. 1(b). The absorption peaks of the graphene were observed at 270 nm for 1-propanol, EtOH and EG, confirming the stable dispersibility of reduced graphene in those solvents.[33] We note that the spectra for NMP, 1,3-dimethyl-2-imidazolidinone, γ-butyrolactone, and DMF were plotted in the wavelength above 269 nm, because it was impossible to compensate their strong absorption below 269 nm.

Fig. 2 shows an AFM image of graphene sheets deposited on a silicon wafer by drop-casting a reduced graphene dispersion in 1,3-dimethyl-2-imidazolidinone. The measured thickness of ~0.91 demonstrates that the reduced graphene is fully exfoliated into individual sheets.[18]

Hansen solubility parameter[34] including δ_d (dispersion cohesion parameter), δ_P (polarity cohesion parameter), and δ_H (hydrogen bonding cohesion parameter) provides very useful

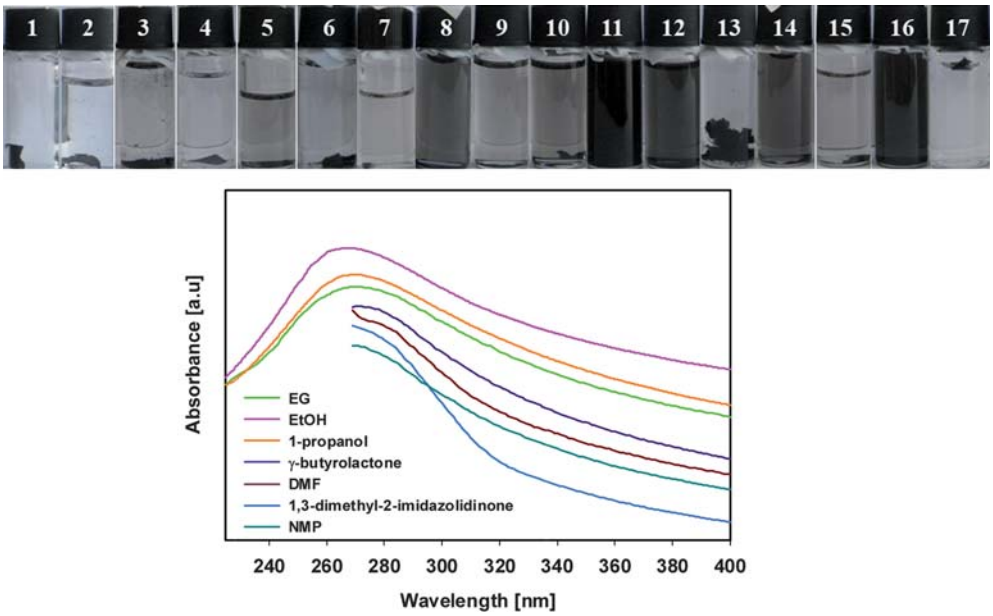

Fig. 1 (a) Photographs of reduced graphene dispersed in water and 16 organic solvents *via* 5 h sonication. The photographs were taken 1 month after the preparation of the reduced graphene dispersion. (b) UV-Vis absorption spectra of reduced graphene dispersed in good solvents. The spectra of NMP, 1,3-dimethyl-2-imidazolidinone, DMF, and γ-butyrolactone are only shown in the wavelength range from 269 nm to 400 nm due to compensation for their strong absorption at <269 nm.

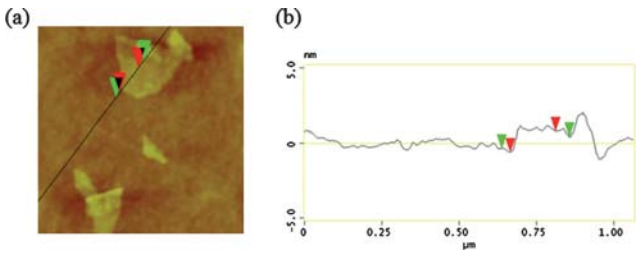

Fig. 2 (a) An AFM image (1 μm × 1 μm) of isolated reduced graphene sheets deposited onto an Si wafer from dispersion in 1,3-dimethyl-2-imidazolidinone, (b) a thickness profile of graphene sheets marked by the black line in (a), where the height differences are 1.77 nm between the two black arrows, 0.91 nm between the two red arrows and 1.24 nm between the two green arrows, respectively.

information to predict dispersibility of graphene in organic solvents.[33] Ruoff and co-workers demonstrated that reduced graphene sheets could be well dispersed in several organic solvents having high $\delta_P + \delta_H$ value.[35] As summarized in Table 1, the organic solvents tested in this study are listed up with $\delta_P + \delta_H$ values. The solvents (NMP, 1,3-dimethyl-2-imidazolidinone, γ-butyrolactone, 1-propanol, DMF, EtOH and EG) had relatively high $\delta_P + \delta_H$ values compared to nonsolvents (hexane, benzene, o-xylene, dichloromethane, THF, pyridine and acetone) for reduced graphene. However, as previously commented by Ruoff ad co-workers, reduced graphene was not dispersable in DMSO, MeOH and water despite their high $\delta_P + \delta_H$. We note that among various nonsolvents for reduced graphene, the small pieces of reduced graphene paper were not even split into smaller pieces in hexane, benzene, dichloromethane or water after 5 h sonication, while they were split into small pieces and swollen in o-xylene, THF, pyridine, acetone, DMSO and MeOH. This indicates that hexane, benzene, dichloromethane and water are highly incompatible to reduced graphene.

Table 1 Dispersibility of reduced graphene in the tested solvents and their 70 Hansen solubility parameters

No.	Solvent	Hansen solubility parameters [MPa$^{1/2}$][32]				Dispersibility of reduced graphene
		δ_D	δ_P	δ_H	$\delta_P + \delta_H$	
1	Hexane	14.9	0.0	0.0	0.0	No
2	Benzene	18.4	0.0	2.0	2.0	No
3	o-Xylene	17.8	1.0	3.1	4.1	No
4	Dichloromethane	18.2	6.3	6.1	12.4	No
5	THF	16.8	5.7	8.0	13.7	No
6	Pyridine	19.0	8.8	5.9	14.7	No
7	Acetone	15.5	10.4	7.0	17.4	No
8	NMP	18.0	12.3	7.2	19.5	Yes
9	1,3-dimethyl-2-imidazolidinone	18.0	10.5	9.7	20.2	Yes
10	γ-butyrolactone	19.0	16.6	7.4	24.0	Yes
11	1-propanol	16.0	6.8	17.4	24.2	Yes
12	DMF	17.4	13.7	11.3	25.0	Yes
13	DMSO	18.4	16.4	10.2	26.6	No
14	EtOH	15.8	8.8	19.4	28.2	Yes
15	MeOH	15.1	12.3	22.3	34.6	No
16	EG	17.0	11.0	26.0	37.0	Yes
17	Water	15.5	16.0	42.3	58.3	No

Noncovalent functionalization of reduced graphene by end-functional polymers

Reduced graphene could be dispersed in nonsolvents through noncovalent grafting with an end-functional polymer, PS–NH_2. Among the various nonsolvents for reduced graphene, hexane, benzene, o-xylene and dichloromethane, which are immiscible with the aqueous phase, were used for the noncovalent functionalization. Fig. 3(a) shows the photograph taken before sonication. In each vial, the dark phase corresponds to the

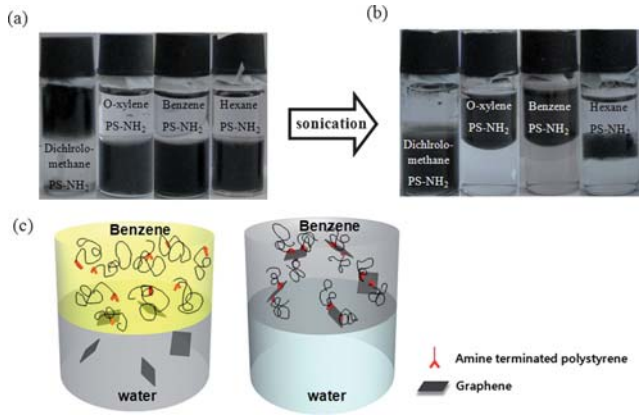

Fig. 3 Phase transfer of reduced graphene (0.009 wt%) from the aqueous phase to the organic phase *via* PS–NH_2 functionalization. (a) Before sonication, dark phases were aqueous dispersions of reduced graphene, and transparent phases were PS–NH_2 (1.3 wt%) dissolved organic solvents. (b) After 5 h sonication, phase transfer occurred, except in hexane. (c) A schematic illustration of phase transfer *via* noncovalent functionalization.

aqueous dispersion of reduced graphene and the transparent phase corresponds to the PS–NH_2 (1.3 wt%) dissolved non-solvents. The aqueous phases with reduced graphene were located at the bottom and the organic phases with PS–NH_2 (transparent phases) were located on the top side for o-xylene (density: 0.879 g ml^{-1}), benzene (density: 0.874 g ml^{-1}) and hexane (density: 0.659 g ml^{-1}), due to their low density. On the other hand, aqueous phase was located on the top side and dichloromethane with PS–NH_2 was at the bottom due to the high density of dichloromethane (density: 1.325 g ml^{-1}). After 5 h sonication, the organic phases except hexane became dark, indicating that the reduced graphene sheets were phase transferred to the organic phases (Fig. 3(b)). A schematic description of the phase transfer is presented in Fig. 3(c).

The reduced graphene was transferred from aqueous to organic phase due to the noncovalent (ionic) interaction between the protonated terminal amine groups (NH_3^+) of PS–NH_2 and carboxylate groups (COO^-) of reduced graphene. As shown in the ATR-FTIR spectra of Fig. 4, the peak for the N–H bending of pure PS–NH_2 at 1600 cm^{-1} became significantly broadened after functionalization to graphene. This confirms that ionic interaction occurred between the protonated terminal amine groups of PS–NH_2 and the carboxylate groups on the graphene sheet.[36] Fig. 5 exhibits dispersive Raman spectra of PS–NH_2 functionalized reduced graphene, reduced graphene, graphene oxide and graphite. The G band of graphene oxide is broadened and shifted from 1567 cm^{-1} to 1596 cm^{-1}, and the D band becomes significantly stronger than graphite.[17] The Raman spectrum of reduced graphene shows higher D/G intensity ratio (1.05) than graphene oxide (0.92) implying the decreased size of the sp^2 domains upon chemical reduction of the graphene oxide.[37] The G band of reduced graphene observed at 1589 cm^{-1} markedly shifted to 1596 cm^{-1} after PS–NH_2 functionalization, indicating a better exfoliation of graphene layers.[38–41] The carboxylate groups of graphitic materials induced by acid-treatment have been used to provide a functionalization sites for amine-containing molecules.[42] Similar noncovalent ionic functionalization of carbon nanotubes was used in our previous work.[41,43–45] In the present work, we demonstrate that the carboxylate groups remaining at reduced graphene after the hydrazine reduction of graphene oxide provide sufficient functionalization sites for PS–NH_2. Furthermore, a high dispersibility in a broad spectrum of organic solvents is anticipated in our approach, owing to the large size and chemical diversity of the polymeric dispersant.[43]

Noncovalent functionalization of reduced graphene in benzene was tested in the presence of various polymers including PS, PMMA–OH, PS–COOH and PS–NH_2, as shown in Fig. 6. The noncovalent functionalization occurred only with PS–NH_2. Other polymers simply caused the dilution of dark water phases without phase transfer. The dilution occurred as reduced graphene sheets moved to the water–benzene interface due to the attractive interactions between reduced graphene in water phase and polymers in benzene phase. However, complete phase transfer did not occur in the absence of amine terminated polymers.

The phase transfer of reduced graphene to the benzene phases with various concentrations of PS–NH_2 is demonstrated in Fig. 7. After 5 h sonication, reduced graphene was well-dispersed in benzene phase containing 0.4 wt% or 0.7 wt% of PS–NH_2, while it remained at the water–benzene interface in other vials

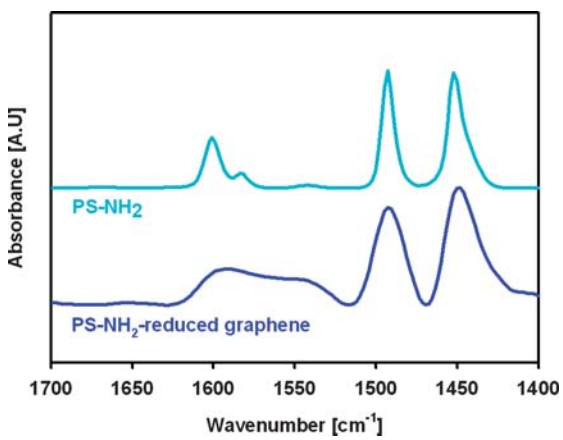

Fig. 4 ATR-FTIR spectra of pure PS–NH_2 and PS–NH_2 functionalized reduced graphene.

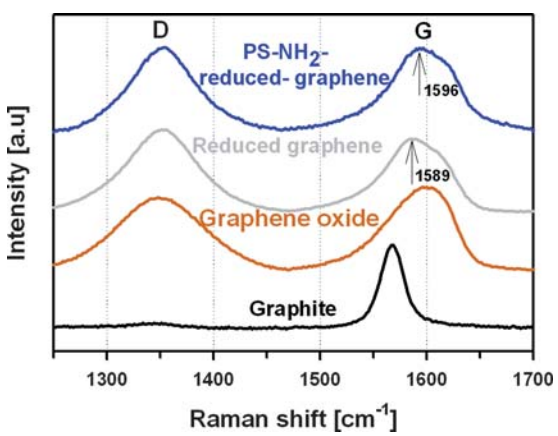

Fig. 5 Dispersive Raman spectra of PS–NH_2 functionalized reduced graphene, reduced graphene, graphene oxide and graphite.

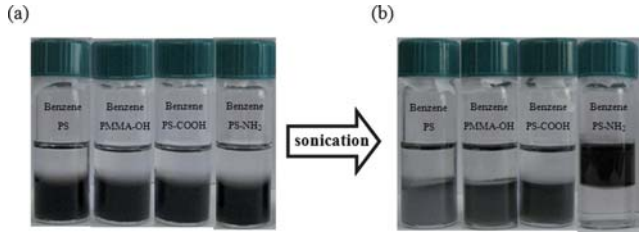

Fig. 6 Photographs for phase transfer of reduced graphene (0.009 wt%) in the presence of various polymers: (a) before and (b) after 5 h sonication. Benzene phases include PS, PMMA–OH, PS–COOH and PS–NH_2 (polymer concentration: 1.3 wt%).

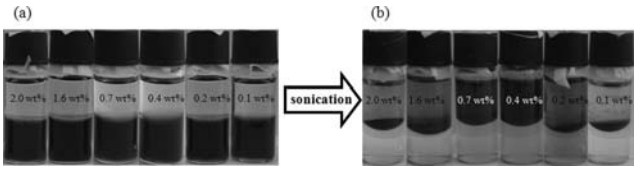

Fig. 7 Photographs for phase transfer of reduced graphene (0.009 wt%) in the presence of various concentrations of PS–NH_2 in benzene phase: (a) before and (b) after 5 h sonication.

(although phase transfer has occurred, reduced graphene has precipitated at the interface). When the concentration of PS–NH_2 is low (0.1 wt% and 0.2 wt%), the insufficient functionalization of reduced graphene may result in the poor dispersibility. Both reduced graphene and PS–NH_2 functionalized reduced graphene sheets are located at water–benzene interface. On the other hand, we presume that the poor dispersibility at high concentration (1.6 or 2.0 wt%) is attributed to the depletion interaction involved with free excess PS–NH_2. As the reduced graphene in benzene phase approached each other, their depletion zones overlapped to generate a volume of solvent between the reduced graphene, where the concentration of the free PS–NH_2 that are unbound to graphene surface was significantly less than that in the bulk solvent. The difference in osmotic pressure between the bulk solvent and the solvent in depletion zone leads to an effective attraction among graphene sheets (depletion interaction), resulting in the observed aggregation of graphene sheets.[46]

Conclusions

A novel method for dispersing graphene in various organic solvents by noncovalent functionalization with end-functional polymers has been demonstrated. The carboxylate groups remaining after chemical reduction of graphene oxide successfully provided the noncovalent functionalization sites to the protonated amine terminal group of end-functional polymers. The noncovalent functionalization facilitated the phase transfer of graphene sheets from water phase to organics phase *via* simple sonication. The chemical nature of organic solvents and the end-functional group of polymer as well as the concentration of end-functional polymer were crucial to determine the functionalizability and dispersibility of reduced graphene. The facile organo-dispersibility of polymer functionalized graphene achieved in the approach demonstrated here opens up a new route to graphene processing, which may broaden the application area of highly functional two-dimensional carbon materials.

Acknowledgements

This work was supported by the National Research Laboratory (NRL) Program (R0A-2008-000-20057-0), and the World Class University (WCU) program (R32-2008- 000-10051-0) funded by the Korean government (MEST).

References

1 K. S. Novoselov, A. K. Geim, S. V. Morozov, D. Jiang, Y. Zhang, S. V. Dubonos, I. V. Grigorieva and A. A. Firsov, *Science*, 2004, **306**, 666.
2 K. Geim and K. S. Novoselov, *Nat. Mater.*, 2007, **6**, 183.
3 S. Gilje, S. Han, K. L. Wang and R. B. Kaner, *Nano Lett.*, 2007, **7**, 3394.
4 F. Schedin, A. K. Geim, S. V. Morozov, E. W. Hill, P. Blake, M. I. Katsnelson and K. S. Novoselov, *Nat. Mater.*, 2007, **6**, 652.
5 J. S. Bunch, A. M. van der Zande, S. S. Verbridge, I. W. Frank, D. M. Tanenbaum, J. M. Parpia, H. G. Craighead and P. L. McEuen, *Science*, 2007, **315**, 490.
6 X. Wang, L. J. Zhi and K. Mullen, *Nano Lett.*, 2008, **8**, 323.
7 Z. Liu, Q. Liu, Y. Huang, Y. Ma, S. Yin, X. Zhang, W. Sun and Y. Chen, *Adv. Mater.*, 2008, **20**, 3924.
8 B. Standley, W. Bao, H. Zhang, J. Bruck, C. N. Lau and M. Bockrath, *Nano Lett.*, 2008, **8**, 3345.
9 J. O. Sofo, A. S. Chaudhari and G. D. Barber, *Phys. Rev. B: Condens. Matter Mater. Phys.*, 2007, **75**, 153401.
10 G. K. Dimitrakakis, E. Tylianakis and G. E. Froudakis, *Nano Lett.*, 2008, **8**, 3166.
11 M. D. Stoller, S. Park, Y. Zhu, J. An and R. S. Ruoff, *Nano Lett.*, 2008, **8**, 3498.
12 C. Berger, Z. M. Song, X. B. Li, X. S. Wu, N. Brown, C. Naud, D. Mayou, T. B. Li, J. Hass, A. N. Marchenkov, E. H. Conrad, P. N. First and W. A. de Heer, *Science*, 2006, **312**, 1191.
13 H. C. Schniepp, J. L. Li, M. J. McAllister, H. Sai, M. Herrera-Alonso, D. H. Adamson, R. K. Prud'homme, R. Car, D. A. Saville and I. A. Aksay, *J. Phys. Chem. B*, 2006, **110**, 8535.
14 J. Coraux, A. T. N'Diaye, C. Busse and T. Michely, *Nano Lett.*, 2008, **8**, 565.
15 A. Dato, V. Radmilovic, Z. H. Lee, J. Phillips and M. Frenklach, *Nano Lett.*, 2008, **8**, 2012.
16 S. Stankovich, R. D. Piner, X. Q. Chen, N. Q. Wu, S. T. Nguyen and R. S. Ruoff, *J. Mater. Chem.*, 2006, **16**, 155.
17 S. Stankovich, R. D. Piner, S. T. Nguyen and R. S. Ruoff, *Carbon*, 2006, **44**, 3342.
18 D. Li, M. B. Muller, S. Gilje, R. B. Kaner and G. G. Wallace, *Nat. Nanotechnol.*, 2008, **3**, 101.
19 S. Park, J. An, R. D. Piner, I. Jung, D. Yang, A. Velamakanni, S. T. Nguyen and R. S. Ruoff, *Chem. Mater.*, 2008, **20**, 6592.
20 X. Fan, W. Peng, Y. Li, X. Li, S. Wang, G. Zhang and F. Zhang, *Adv. Mater.*, 2008, **20**, 4490.
21 Y. Hernandez, V. Nicolosi, M. Lotya, F. M. Blighe, Z. Sun, S. De, I. T. McGovern, B. Holland, M. Byrne, Y. K. Gun'ko, J. J. Boland, P. Niraj, G. Duesberg, S. Krishnamurthy, R. Goodhue, J. Hutchison, V. Scardaci, A. C. Ferrari and J. N. Coleman, *Nat. Nanotechnol.*, 2008, **3**, 563.
22 L. M. Viculis, J. J. Mack and R. B. Kaner, *Science*, 2003, **299**, 1361.
23 M. V. Savoskin, V. N. Mochalin, A. P. Yaroshenko, N. I. Lazareva, T. E. Konstantinova, I. V. Barsukov and I. G. Prokofiev, *Carbon*, 2007, **45**, 2797.
24 O. Lerf, H. He, M. Forster and J. Klinowski, *J. Phys. Chem. B*, 1998, **102**, 4477.
25 T. Szabo, O. Berkesi, P. Forgo, K. Josepovits, Y. Sanakis, D. Petridis and I. Dekany, *Chem. Mater.*, 2006, **18**, 2740.
26 H. He, J. Klinowski, M. Forster and A. Lerf, *Chem. Phys. Lett.*, 1998, **287**, 53.
27 C. Hontoria-Lucas, A. J. López-Peinado, J. de D. López -González, M. L. Rojas-Cervantes and R. M. Martín-Aranda, *Carbon*, 1995, **33**, 1585.

28 S. Niyogi, E. Bekyarova, M. E. Itkis, J. L. McWilliams, M. A. Hamon and R. C. Haddon, *J. Am. Chem. Soc.*, 2006, **128**, 7720.
29 Y. Liang, D. Wu, X. Feng and K. Müllen, *Adv. Mater.*, 2009, **21**, 1679.
30 S. Stankovich, D. A. Dikin, G. H. B. Dommett, K. M. Kohlhaas, E. J. Zimney, E. A. Stach, R. D. Piner, S. T. Nguyen and R. S. Ruoff, *Nature*, 2006, **442**, 282.
31 T. Ramanathan, A. A. Abdala, S. Stankovich, D. A. Dikin, M. Herrera-alonso, R. D. Piner, D. H. Adamson, H. C. Schniepp, X. Chen, R. S. Ruoff, S. T. Nguyen, I. A. Aksay, R. K. Prud'homme and L. C. Brinson, *Nat. Nanotechnol.*, 2008, **3**, 327.
32 W. S. Hummers and R. E. Offeman, *J. Am. Chem. Soc.*, 1958, **80**, 1339.
33 J. I. Paredes, S. Villar-Rodil, A. Martínez-Alonso and J. M. D. Tascón, *Langmuir*, 2008, **24**, 10560.
34 C. M. Hansen, *Hansen Solubility Parameters: A User's Handbook*, CRC Press, Hoboken, 2nd edn, 2007.
35 S. Park, J. An, I. Jung, R. D. Piner, S. J. An, X. Li, A. Velamakanni and R. S. Ruoff, *Nano Lett.*, 2009, **9**, 1593.
36 M. Bieri and T. Bürgi, *Langmuir*, 2006, **22**, 8379.
37 F. Tuinstra and J. L. Koenig, *J. Chem. Phys.*, 1970, **53**, 1126.
38 S. Qin, D. Qin, W. T. Ford, J. E. Herrera and D. E. Resasco, *Macromolecules*, 2004, **37**, 9963.
39 C. Stephan, T. P. Nguyen, M. L. de la Chapelle, S. Lefrant, C. Journet and P. Bernier, *Synth. Met.*, 2000, **108**, 139.
40 O. M. Rao, J. Chen, E. Richter, U. Schlecht, P. C. Eklund, R. C. Haddon, U. D. Venkateswaran, Y. K. Kwon and D. Tomanek, *Phys. Rev. Lett.*, 2001, **86**, 3895.
41 S. H. Lee, J. S. Park, B. K. Lim and S. O. Kim, *J. Appl. Polym. Sci.*, 2008, **110**, 2345.
42 M. A. Hamon, J. Chen, H. Hu, Y. Chen, M. E. Itkis, A. M. Rao, P. C. Eklund and R. C. Haddon, *Adv. Mater.*, 1999, **11**, 834.
43 S. H. Lee, J. S. Park, J. M. Koo, B. K. Lim and S. O. Kim, *Macromol. Res.*, 2008, **16**, 261.
44 S. H. Lee, J. S. Park, B. K. Lim, C. B. Mo, W. J. Lee, J. M. Lee, S. H. Hong and S. O. Kim, *Soft Matter*, 2009, **5**, 2343.
45 D. H. Lee, W. J. Lee and S. O. Kim, *Nano Lett.*, 2009, **9**, 1427.
46 R. A. L. Jones, *Soft Condensed Matter*, Oxford University Press, Oxford, 2002.

